

Received May 17, 2013; reviewed; accepted July 15, 2013

INFLUENCE OF CALCINATION PARAMETERS ON PHYSICOCHEMICAL AND STRUCTURAL PROPERTIES OF CO-PRECIPIATED MAGNESIUM SILICATE

Filip CIESIELCZYK*, Przemysław BARTCZAK*, Lukasz KLAPISZEWSKI*,
Dominik PAUKSZTA*, Adam PIASECKI**, Teofil JESIONOWSKI*

* Poznan University of Technology, Faculty of Chemical Technology, Institute of Chemical Technology and Engineering, M. Skłodowskiej-Curie 2, PL-60-965, Poznan, Poland, Filip.Ciesielczyk@put.poznan.pl

** Poznan University of Technology, Faculty of Mechanical Engineering and Management, Institute of Materials Science and Engineering, Jana Pawła II 24, PL-60-965, Poznan, Poland

Abstract: Physicochemical properties of different oxide systems depend mostly on the method of their preparation and classification, so the main aim of the study was to obtain the MgO·SiO₂ hybrid in an aqueous solution and its calcination under assumed conditions. Research scope included evaluation of the effect of the basic parameters of the calcination process (time and temperature) on the structural properties of the final materials. Products obtained by the proposed method were thoroughly characterized. The chemical composition, crystalline structure, morphology and nature of the dispersion as well as parameters of the porous structure were established. The results of research in a decisive manner confirmed the possibility of designing the properties of inorganic oxide systems such as MgO·SiO₂, which will definitively be scheduled into potential directions for their use.

Keywords: *magnesium silicate, precipitation, calcination, WAXS, porous structure*

Introduction

Naturally occurring oxide materials are the largest group of minerals that create the Earth's crust. They are among the most important mineral resources, both in terms of quantity and availability of their deposits. Such systems are becoming increasingly applied in terms of technological and economic development. Thanks to its unique physicochemical properties they are used in many industries. They have become the basic raw material for ceramics, paints, lacquers, plastics and bioceramics (Qiu, 2013; Johnson, 2004; Lu, 2012).

Today's technology is gaining more and more interest in oxide materials obtained in the laboratory. Synthetic powders may have similar or quite different properties in

comparison to their natural substituents. The use of synthetic oxide materials is increasing and is a result of the ability to control and improvement of their physicochemical properties (Baldyga, 2012; Modrzejewska-Sikorska, 2012; Laurentowska, 2012; Yamagata, 2013). These properties depend mostly on the preparation process parameters, such as concentration of reagents, the direction and speed of dosing, temperature and pH. In addition, synthetic powders can be subjected to numerous chemical modifications, changing the spectrum of a wide range of application. The modification is carried out with the use of a large group of organic compounds which provide products with specific hydrophilic-hydrophobic properties and surface activity (Bhardwaj, 2012, Zhang, 2013). In addition to these processes, important is the final step of oxide materials classification, including thermal treatment (calcination). Selection of the calcination process parameters of these powders is important from the point of view of porous structure, hydrophilic-hydrophobic nature, crystalline structure and dispersion characteristics (Ibrahim, 2012; Ren, 2013; Saruchi, 2013).

The calcination process is generally carried out at a temperature lower than the melting point of the calcinated product. In various research papers the influence of calcination on the physicochemical properties of oxide materials was described so far. Choi et al. (2012) have shown that the structure of mesoporous (granular) systems of titanium dioxide and aluminum oxide ($\text{TiO}_2/\text{Al}_2\text{O}_3$) can be easily controlled by calcination temperature and the ratio of reagents. The calcination was carried out at three different temperatures: 450, 600 and 750 °C. It was found that the higher the calcination temperature the pore size increases and the volume as well as the bending strength slightly decrease, which directly translates to surface area development. Other researchers (Yu, 2006) have proved that the calcination process affects morphology, surface area, structure and photocatalytic properties of titanium nanotubes. Titanium nanotubes calcinated in the temperature range 400–600 °C had a larger surface area and greater pore volume than the starting material. A further increase in calcination temperature (700–900 °C) caused a decrease in photocatalytic properties and pore volume, reduction of the surface area, as a result of the formation of the rutile structure. Mohammadi et al. (2003) conducted a study on the effect of calcination of kaolin used for zeolite membranes. It was found that an increase in the calcination temperature improves the strength properties of kaolin, which is caused by the formation of the two forms of the compound above 1000 °C – mullite and spinel and the increase in pore diameter. In other work (Guo, 2010), calcination process at four different temperatures (200–500 °C) and five different times (1–5 h) was realized for sodium silicate, in order to obtain a product characterized with the best properties for biodiesel production (sodium silicate acted as the solid catalyst of the transesterification process). The optimum calcination condition of Na_2SiO_3 for biodiesel production from soybean oil was at temperature of 400 °C and calcination duration – 2 h. In subsequent scientific reports Yan et al. (2010) studied the effect of temperature of calcination process in the production of calcium sorbents. Best results were obtained at 503 °C to

607 °C as a process temperature. Tangchupong and co-authors (2010) studied the effect of calcination temperature on the properties of sulfated zirconia – commercial and synthetic obtained via precipitation method. It has been shown that change in the calcination temperature from 450 °C to 750 °C significantly influences surface properties, and also the acid-base character of the surface of such systems. Using a commercial product in the conversion of carbon monoxide, it was found that the reaction rate decreases with increasing calcination temperature. For the product precipitated and calcinated in the temperature range of 450–600 °C, the conversion of CO increased, and after calcination at 750 °C it decreased.

Calcination process is gaining importance in area of today's technology, giving the ability to control the physicochemical properties of calcinates (moisture content, sorption capacity, diameter and pore volume, surface activity, the hydrophilic-hydrophobic character), resulting in subsequent directions of their use, despite various costly modifications with other compounds.

Experimental

Synthesis of MgO·SiO₂ powder and its calcination

The magnesium silicate powder was obtained in a process of precipitation from aqueous solutions of sodium silicate and magnesium sulfate, as described earlier (Ciesielczyk, 2011). Precipitation of MgO·SiO₂ powder was realized in the QVF Mini Plant Pilot-Tec reactor having 10 dm³ capacity, equipped with a high speed stirrer (2000 rpm). Five dm³ of 5% magnesium sulfate solution was previously placed in the reactor. After that, the 5% solution of sodium silicate in appropriate amount was dosed to the reactor (1 dm³/h) using a peristaltic PP2B-15 pump. The product obtained – MgO·SiO₂ in a form of white powder – was washed and filtrated, and then dried at 105 °C for 24 h. The prepared powders were additionally calcinated, using a Controller P320 oven made by Nabertherm, at 300, 450, 600, 750, 900 and 1000 °C. For each of these temperatures of calcinations, the process lasted for 1 and 2 h, respectively.

Physicochemical properties evaluation

The dispersive characteristic of the MgO·SiO₂ oxide material and its calcinates was determined using a Mastersizer 2000 apparatus made by Malvern Instruments Ltd., by using the laser diffraction method and measuring particles of sizes from 0.2 to 2000 μm. The morphology and microstructure of the materials obtained were analyzed using a Zeiss EVO40 scanning electron microscope. The observations permitted evaluation of the dispersion degree, the structure of particles and their tendency towards aggregation or agglomeration. Moreover, the surface composition of calcinates (contents of Mg, Si and O) was analyzed by energy dispersive X-Ray spectroscopy (EDS) using a Princeton Gamma-Tech unit equipped with a prism digital

spectrometer. The calcinates of $\text{MgO}\cdot\text{SiO}_2$ were also subjected to crystalline structure determination using the WAXS method. The results were analyzed employing a XRAYAN software. The diffraction patterns were taken using a TUR-M62 horizontal diffractometer equipped with an HZG-3 type goniometer. The surface area A_{BET} (BET method) was calculated based on data measured by low-temperature adsorption of nitrogen. The isotherms of nitrogen adsorption/desorption were measured at $-196\text{ }^\circ\text{C}$ using an ASAP 2020 apparatus made by Micromeritics Instrument Co. With regard to the high accuracy of the instrument used ($\pm 0.0001\text{ m}^2/\text{g}$) the surface area values were rounded up to interger numbers, and the mean pore size (S_p) and total pore volume (V_p), calculated using the BJH algorithm, were rounded to one and two decimal places respectively.

Results and discussion

Dispersive and morphological characteristics of $\text{MgO}\cdot\text{SiO}_2$ calcinates

In the first stage of study, the dispersion characteristics and morphology of the obtained $\text{MgO}\cdot\text{SiO}_2$ calcinates were established. Table 1 shows the dispersive parameters, and Figure 1 shows SEM images of the precipitated powder, additionally calcinated at different temperatures. The data indicate that the largest average particle diameter ($25.9\text{ }\mu\text{m}$) was in sample PB 0, that was not calcinated $\text{MgO}\cdot\text{SiO}_2$. The largest volume contribution (4.9%) in this sample is represented by the particles of $39.8\text{ }\mu\text{m}$ in diameter. This sample contains 10% of the particles having a diameter less than $3.6\text{ }\mu\text{m}$, 50% of the particles having a diameter less than $18.0\text{ }\mu\text{m}$ and 90% of particles smaller than $60.7\text{ }\mu\text{m}$. The SEM image of this sample shows particles smaller than $10\text{ }\mu\text{m}$, as well as the bigger ones, which directly confirms the obtained particle sizes (see Fig. 1a). Sample PB 7 calcinated at $750\text{ }^\circ\text{C}$, PB 3 calcinated at $450\text{ }^\circ\text{C}$ and PB 1 calcinated at $300\text{ }^\circ\text{C}$ show the most similar nature of dispersion as compared to the not calcinated sample, which is evidenced by the values of $d(0.1)$ $d(0.5)$ $d(0.9)$ parameters, as well as by the average particle diameter in the range of $21.6\text{--}22.5\text{ }\mu\text{m}$. The smallest particle sizes were obtained in sample PB 11 calcinated at $1000\text{ }^\circ\text{C}$. Its average particle diameter in hole volume of the sample is $14.8\text{ }\mu\text{m}$. Other samples were characterized by similar values of individual parameters falling within the range of $d(0.1) = 18.1\text{--}18.7\text{ }\mu\text{m}$, $d(0.5) = 12.4\text{--}13.0\text{ }\mu\text{m}$ and $d(0.9) = 40.1\text{--}42.8\text{ }\mu\text{m}$.

Carrying out the process of calcination for 2 h, it was found that the largest average particle diameter in the entire volume of the sample has a powder calcinated at $1000\text{ }^\circ\text{C}$ (PB 12) – $24.6\text{ }\mu\text{m}$. Samples characterized with the smallest particle sizes were those calcinated at $750\text{ }^\circ\text{C}$ (PB 8) – $12.1\text{ }\mu\text{m}$ and at $300\text{ }^\circ\text{C}$ (PB 2) – $12.8\text{ }\mu\text{m}$. Other samples were characterized by similar dispersion parameters ($d(0.1) = 3.1\text{--}3.2\text{ }\mu\text{m}$, $d(0.5) = 11.3\text{--}13.7\text{ }\mu\text{m}$ and $d(0.9) = 36.7\text{--}45.8\text{ }\mu\text{m}$). The average particle diameter for samples PB 10, PB 6 and PB 4 are respectively 19.9 , 18.8 and $16.5\text{ }\mu\text{m}$.

Analyzing the results concerning the characteristics of the dispersion and morphology it was proved that calcination process contributes to significant changes

in these properties. Change in the size of the particles (the nature of the dispersion) is determined by the temperature and time of calcination. The most significant changes were observed when comparing the $\text{MgO}\cdot\text{SiO}_2$ powder calcinated at $750\text{ }^\circ\text{C}$ and $300\text{ }^\circ\text{C}$, however, definitely the best dispersive-morphological parameters have calcinates obtained in a 2-hours calcination process. Experimental data are confirmed by Fig. 1. The scanning electron microscopy images of selected calcinates are analogous to the data presented in the literature concerning the thermal treatment of other precipitated powders (Kim, 2002).

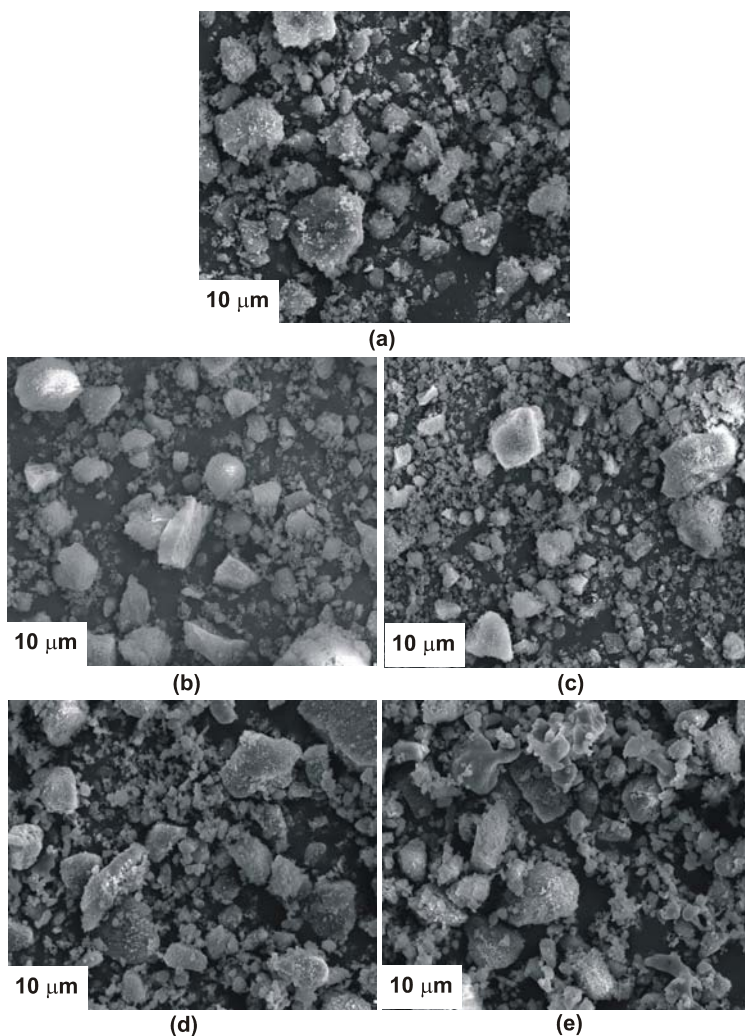


Fig. 1. SEM images of $\text{MgO}\cdot\text{SiO}_2$ powder (a) without calcination, (b) and (c) calcinated at $450\text{ }^\circ\text{C}$ and (d) and (e) calcinated at $1000\text{ }^\circ\text{C}$ for 1 or 2 h, respectively

Table 1. Dispersive parameters of MgO·SiO₂ powder calcinated at different temperatures

Sample symbol	Calcination temperature (°C)	Calcination time (h)	Diameter (μm)			
			<i>D</i> (4.3)	<i>d</i> (0.1)	<i>d</i> (0.5)	<i>d</i> (0.9)
PB 0	–	–	25.9	3.6	18.0	60.7
PB 1	300	1	22.2	3.4	14.8	51.8
PB 3	450		22.5	3.4	15.0	52.9
PB 5	600		18.7	3.1	12.4	42.8
PB 7	750		21.6	3.2	15.2	49.6
PB 9	900		18.1	3.1	13.0	40.1
PB 11	1000		14.8	3.6	12.4	29.2
PB 2	300	2	12.8	2.7	7.1	21.7
PB 4	450		16.5	3.1	11.3	36.7
PB 6	600		18.8	3.2	12.6	43.0
PB 8	750		12.1	2.7	8.1	23.1
PB 10	900		19.9	3.1	13.7	45.8
PB 12	1000		24.6	5.6	20.1	50.5

Chemical composition of calcinates

Table 2 shows the results of EDS analysis of the calcinates received after 1-hour calcination, which confirms the presence of characteristic elements present in the structure of MgO·SiO₂ powder. The presented experimental data proved that together with an increase in the calcination temperature the mass contribution of magnesium and silicon, which are part of material structure, slightly increases.

Table 2. Chemical composition of MgO·SiO₂ powder calcinated at different temperatures for 1 h

Element	Mass contribution (%)						
	PB 0	PB 1	PB 3	PB 5	PB 7	PB 9	PB 11
Mg	8.02	8.12	8.08	8.27	8.32	8.45	8.56
Si	35.59	34.55	34.72	36.88	36.87	36.99	37.99
Na	1.29	0.89	1.05	1.10	0.98	1.11	0.97
K	0.03	0.02	0.03	0.03	0.03	0.03	0.02
Ca	0.01	0.01	0.01	0.01	0.01	0.01	0.01
O	55.06	56.99	54.88	54.32	53.86	53.08	52.34

The presence in the structure of MgO·SiO₂ such elements as sodium, potassium or calcium is a result of composition of raw materials, especially of sodium silicate solution, used in the synthesis process. However, the oxygen content is slightly reduced, which is directly associated with the constitutional water loss, released during calcination, especially at higher temperatures. Calcination of the powder, performed for 2 h, gave analogous results.

WAXS analysis

In order to compare the crystalline structures of $\text{MgO}\cdot\text{SiO}_2$ powders calcinated at different temperatures for 1 and 2 h, Fig. 2 shows their XRD patterns. As a reference the sample of noncalcinated material was used. Analyzing collected data it was found that with increasing calcination temperature, regardless of time, the crystalline structure of the material is changing. The transition from amorphous to crystalline form occurs not earlier than at $750\text{ }^\circ\text{C}$. The well-defined crystalline structure was obtained in the case of the samples calcinated at high temperature – $1000\text{ }^\circ\text{C}$ (samples PB 11 and PB 12), both for 1 h and 2 h. However, samples calcinated at $900\text{ }^\circ\text{C}$ (samples PB 9 and PB 10) and $750\text{ }^\circ\text{C}$ (sample PB 7 and PB 8) have not fully formed crystalline structure. In the case of the other samples, there was no characteristic diffraction peaks, indicating an amorphous structure of the tested powders. Identification of the diffraction patterns obtained using X-RAYAN software, demonstrated that the diffraction peaks for selected calcinates appear at values of 2θ ranging sequentially 22.06, 28.45, 31.26, 36.05 and 57.09, which clearly indicate the appearance of the synthetic cristobalite (SiO_2) structure in obtained powders.

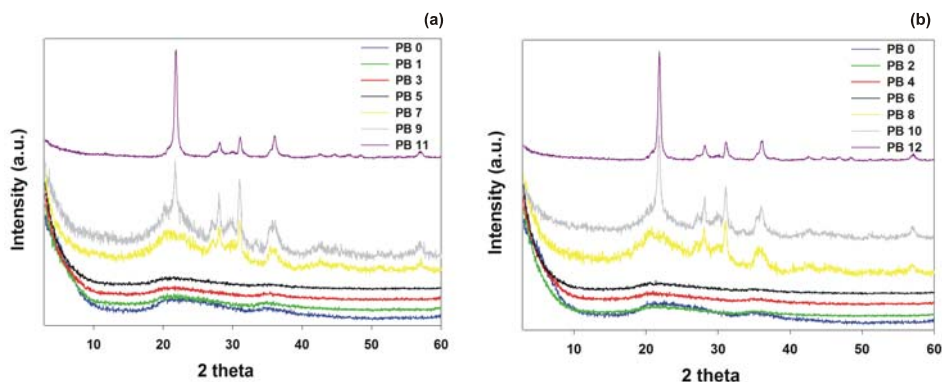


Fig. 2. WAXS patterns of $\text{MgO}\cdot\text{SiO}_2$ calcinates obtained for (a) 1 h and (b) 2 h calcination at different temperatures

Analyzing the obtained results it was found that the calcination process plays a crucial role in changing of the crystalline structure, which is better formed at higher temperatures of the process. This is analogous to the calcination process of selected powders such as TiO_2 . In the case of such monoxide or its mixture ($\text{TiO}_2\cdot\text{SiO}_2$), calcination temperature determines the variation of its crystalline structure. Calcination of these materials at temperature below $700\text{ }^\circ\text{C}$ leads to anatase and the thermal treatment above this temperature results in forming of rutile (Lee, 2007; Siwińska-Stefańska, 2011). These aspects are also correlated with the properties of the obtained materials based on TiO_2 , which determines their potential directions of use.

Porous structure properties

The next step was to determine the parameters of the porous structure of MgO·SiO₂ calcinates. Figure 3 shows the isotherms of nitrogen adsorption/desorption of the MgO·SiO₂ powder calcinated at different temperatures for 1 h and 2 h. The isotherms indicate that the calcination process conditions have an important impact on the parameters of the porous structure. Significant changes were observed in the case of calcinates received at different temperatures of calcination process. However, no significant changes were noted comparing the samples prepared at the same temperatures but at a different time of calcination. The nature of the isotherms obtained indicates the mesoporous character of obtained powders.

For not calcinated sample (PB 0) as well as for calcinates obtained at 300, 450 and 600 °C it was observed that the amount of nitrogen adsorbed slowly increases up to a value of relative pressure equals 0.8. After that the amount of nitrogen adsorbed increases rapidly. For sample not calcinated amount of nitrogen adsorbed at $p/p_0 = 1$ reaches a value of 345 cm³/g. For samples calcinated at temperatures of 300, 450 and 600 °C, this values does not differ in any significant way and are in the range of 305-335 cm³/g (at $p/p_0 = 1$). However, for the samples calcinated at higher temperatures, the difference in the amounts of adsorbed nitrogen is very large. The samples calcinated at 750 °C adsorbed almost half of the amount of nitrogen (210 cm³/g) than the not calcinated sample. The smallest amount of nitrogen adsorbed was observed in the case of the MgO·SiO₂ samples calcinated at 900 and 1000 °C. These values were 60, 40, 15 and 10 cm³/g, respectively.

As in the case of amount of nitrogen adsorbed, the calcination temperature significantly affected the changes in the basic parameters of the porous structure, such as surface area and pore volume and diameter. It was noted that the surface area of obtained powders decreases with increasing temperature of the calcinations process. The largest surface area of 427 m²/g was reached for not calcinated material. However, the largest surface area from all of the analyzed calcinates was obtained for sample PB 11 – 399 m²/g. As the calcination temperature increases the surface area gradually decreases up to the lowest value for powders obtained after calcination of MgO·SiO₂ at 1000 °C. The value of surface area (A_{BET}) is 6 m²/g for the sample calcinated at this temperature for 1 h and 4 m²/g - calcinated for 2 h. Extension of calcination time resulted in a further, slight decrease in the individual parameters of the porous structure. Noteworthy is also the fact that the calcination temperature increase resulted in a decrease of the pore volume from 0.49 and 0.51 cm³/g, respectively, for samples PB 1 and PB 2 (calcinated at 300°C) to a value of 0.02 and 0.01 cm³/g for samples PB 11 and PB 12 calcinated at 1000 °C respectively. Moreover, the pore diameter increases with increasing calcination temperature only up to 750 °C. Above this temperature the pore diameter changes are completely random.

Once again, it was confirmed that the implementation of the calcination of MgO·SiO₂ under certain conditions, led to significant changes in the physicochemical properties of obtained powders. As a confirmation, a number of scientific literature

reports can be used (Choi, 2012; Yu, 2006), which show that too high temperature of calcination reduces the activity of the prepared products and causes a significant reduction in the value of individual parameters of the porous structure.

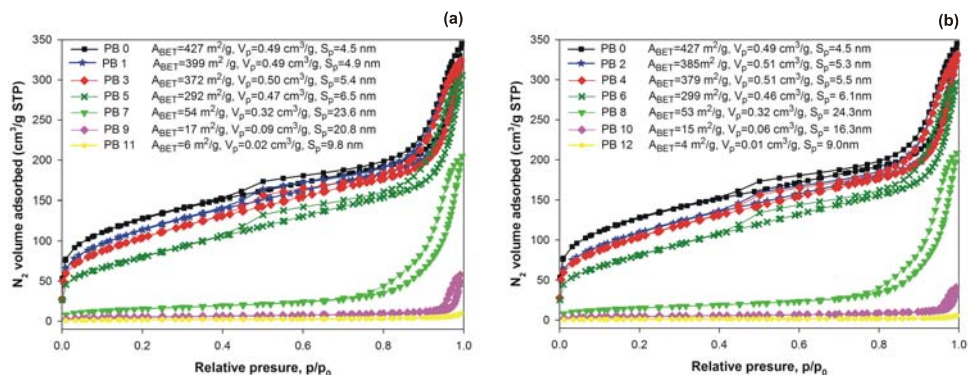


Fig. 3. Characteristics of the porous structure of MgO·SiO₂ powder calcinated for (a) 1 h and (b) 2 h at different temperatures

Conclusions

The study demonstrated that the process of heat treatment of the MgO·SiO₂ powder, implemented via calcination, is a very effective method to change their physicochemical and structural properties. The dispersive characteristics of obtained calcinates depend mainly on the temperature and time of calcination. All powders were characterized with a smaller particle size as compared to not calcinated sample. Insignificant changes were observed while analyzing the chemical composition of the prepared products. The only dependency that was observed was the increase in the percentage contribution of magnesium and silicon in relation to oxygen in the structure of calcinates obtained at higher temperatures.

Calcination of precipitated magnesium silicate at temperatures above 750 °C led to the formation of the crystalline structure corresponding to the structure of synthetic cristobalite. Formation of this structure was noted in the case of calcinates obtained during thermal treatment, implemented at 1000 °C, regardless of the time of calcination. Samples of MgO·SiO₂ calcinated at temperatures below 750 °C were of typical amorphous form.

A significant change in various parameters of the porous structure of obtained powders was also observed, depending on the calcination temperature. It was found that the surface area and pore volume decrease with increasing temperature of the process, while the pore diameter increased only for samples calcinated at temperatures up to 750 °C. Above this temperature changes of this parameter were completely random. The best parameters of the porous structure were exhibited by the system that

was not calcinated ($A_{\text{BET}} = 427 \text{ m}^2/\text{g}$, $V_p = 0.49 \text{ cm}^3/\text{g}$, $S_p = 4.5 \text{ nm}$), whereas the worst by $\text{MgO}\cdot\text{SiO}_2$ calcinated at $1000 \text{ }^\circ\text{C}$ ($A_{\text{BET}} = 4 \text{ m}^2/\text{g}$, $V_p = 0.01 \text{ cm}^3/\text{g}$, $S_p = 9.0 \text{ nm}$).

Acknowledgements

The study was financed within the Polish National Centre of Science funds according to decision no. DEC-2011/03/D/ST5/05802.

References

- BALDYGA J., JASINSKA M., JODKO K., PETELSKI P., 2012, *Precipitation of amorphous colloidal silica from aqueous solutions-aggregation problem*, Chem. Eng. Sci., 77, 207–216.
- BHARDWAJ D., SHARMA M., SHARMA P., TOMAR R., 2012, *Synthesis and surfactant modification of clinoptilolite and montmorillonite for the removal of nitrate and preparation of slow release nitrogen fertilizer*, J. Hazard. Mater., 227–228, 292–300.
- CHOI J., KIM J., YOO K.S., LEE T.G., 2008, *Synthesis of mesoporous $\text{TiO}_2/\gamma\text{-Al}_2\text{O}_3$ composite granules with different sol composition and calcinations temperature*, Powder Technol., 181, 83–88.
- CIESIELCZYK, F., NOWACKA, M., PRZYBYLSKA, A., JESIONOWSKI, T., 2011, *Dispersive and electrokinetic evaluations of alkoxyxilane-modified $\text{MgO}\cdot\text{SiO}_2$ oxide composite and pigment hybrids supported on it*, Colloids Surf. A: Physicochem. Eng. Asp., 376, 21–30.
- GUO F., PENG Z.G., DAI J.Y., XIU Z.L., 2010, *Calcinated sodium silicate as soil base catalyst for biodisel production*, Fuel Process. Technol., 91, 322–328.
- IBRAHIM S.S., SELIM A.Q., 2012, *Heat treatment of natural diatomite*, Physicochem. Probl. Miner. Process., 48, 413–424.
- JOHNSON J.H., MCFARLANE A.J., BORMANN T., MORAES J., 2004, *Nano-structured silica and silicates: new materials and their applications in paper*, Cur. Appl. Phys., 4, 411–414.
- KIM D.J., HAHN S.H., OH S.H., KIM E.J., 2002, *Influence of calcination temperature on structural and optical properties of TiO_2 thin films prepared by sol-gel dip coating*, Mat. Lett., 57, 355–360.
- LAURENTOWSKA A., JESIONOWSKI T., 2012, *$\text{ZnO}\cdot\text{SiO}_2$ oxide composites synthesis during precipitation from emulsion system*, Physicochem. Probl. Miner. Process., 48, 63–76.
- LEE C.-K., WANG C.-A., LYU M.-D., JUANG L.-C., LIU S.-S., HUNG S.-H., 2007, *Effects of sodium content and calcination temperature on the morphology, structure and photocatalytic activity of nanotubular titanates*, J. Colloid Interface Sci., 316, 562–569.
- LU B.-Q., ZHU Y.-J., AO H.-Y., QI C., CHEN F., 2012, *Synthesis and characterization of magnetic iron oxide/calcium silicate mesoporous nanocomposites as a promising vehicle for drug delivery*, Appl. Mater. Interfaces, 4, 6969–6974.
- MODRZEJEWSKA-SIKORSKA A., CIESIELCZYK F., JESIONOWSKI T., 2012, *Synthesis and characterisation of precipitated $\text{CuO}\cdot\text{SiO}_2$ oxide composites*, Pigm. Resin Technol., 41, 71–80.
- MOHAMMADI T., PAK A., 2003, *Effect of calcinations temperature of kaolin as a support for zeolite membranes*, Sep. Purif. Technol., 30, 241–249.
- QIU Z.-Y., NOH I.-S., ZHANG S.-M., 2013, *Silicate-doped hydroxyapatite and its promotive effect on bone mineralization (review)*, Front. Mater. Sci., 7, 40–50.
- REN C., QIU W., CHEN Y., 2013, *Physicochemical properties and photocatalytic activity of the $\text{TiO}_2/\text{SiO}_2$ prepared by precipitation method*, Sep. Purif. Technol., 107, 264–272.
- SARUCHI, SURBHI, AGHAMKAR, P., KUMAR S., 2013, *Neodymia-silica nanocomposites: synthesis and structural properties*, Adv. Mater. Lett., 4, 78–81

- SIWINSKA-STEFANSKA K., PAUKSZTA D., JESIONOWSKI T., 2011, *Physicochemical properties of TiO₂/SiO₂ oxide composites produced by nucleation of reaction system*, Przem. Chem. 90, 1009–1010.
- TANGCHUPONG N., KHAODEE W., JONGSOMJIT B., LAOSIRIPOJAN N., PRASERTHDAM P., ASSABUMRUNGRAT S., 2010, *Effect of calcination temperature on characteristic of sulfated zirconia and it's application as catalyst for isosynthesis*, Fuel Process. Technol., 91, 121–126.
- YAMAGATA C., ELIAS D.R., PAIVA M.R.S., MISSO A.M., CASTANHO S.R.H.M., 2013, *Facile preparation of apatite-type lanthanum silicate by a new water-based sol-gel process*, Mater. Res. Bull., 48, 2227–2231.
- YAN CH.F., GRACE J.R., LIM C.J., 2010, *Effects of rapid calcinations on properties of calcium based sorbents*, Fuel Process. Technol., 91, 1678–1686
- YU J., YU H., CHENG B., TRAPALIS C., 2006, *Effects of calcinations temperature on the microstructures and photocatalytic activity of titanate nanotubes*, J. Mol. Catal., 249, 135–142.
- ZHANG J., GUO Z., ZHI X., TANG H., 2013, *Surface modification of ultrafine precipitated silica with 3-methacryloxypropyltrimethoxysilane in carbonization process*, Colloids Surf. A: Physicochem. Eng. Asp., 418, 174–179.